Effect of Thermal History on Gas Transport in Atactic Polystyrene

Hisashi ODANI, Norio NAGATA, Nobu KITAMURA, Norio NEMOTO, and Michio KURATA*

Films of an atactic polystyrene were given two different thermal histories by treating them under different conditions, and effect of the thermal history was studied by measurements of gas transport parameters and mechanical relaxation behavior. After having been treated at 130°C for 2 hrs, (A) the polymer films were simply quenched to room temperature, the quenched sample, and (B) the films were annealed at 85°C for 10 days, the annealed sample. The permeability and time-lag experiments were made using helium, argon, krypton, and methane as penetrants in the temperature region from 23 to 130°C. Permeation and diffusion behavior of helium was found to be independent of the thremal history. In transport behavior of argon and krypton major change caused by the subsequent annealing was decrease of permeability and diffusion coefficients, while for methane transport these coefficients increased by the subsequent annealing. For all systems investigated a clear break in the Arrhenius plots of diffusion coefficient was found at the glass transition temperature T_g, and activation energies for diffusion were greater above T_g than were below T_g. Furthermore, for diffusion of argon, krypton, and methane in the annealed sample, another break was exhibited in the plots at temperatures T_b which are close to the so-called β transition of polystyrene. Activation energies for diffusion below T_b were smaller than those above T_b. A discontinuity was observed at T_g in the Arrhenius plots for solution of argon, kryton, and methane, while solubility coefficients for helium were found to be constant in the whole temperature range studied. Thermodynamic parameters for gas transport and solution were evaluated, and mechanisms of gaseous diffusion and solution were discussed. At temperatures from 30 to 100°C the quenched sample exhibited a higher loss tangent than the annealed sample. The interpretation of the combined results suggests that the subsequent annealing process may involve the redistribution of the size of the fluctuating free volume elements, which is comparable to that of the larger penetrant species.

KEY WORDS: Quenching/ Annealing/ Permeation/ Diffusion coefficient/ Solubility coefficient/ Activation energy for diffusion/ Mechanical relaxation/ Free volume/

INTRODUCTION

It is well established that polymers are not in thermodynamic equilibrium at temperatures below their glass transition temperature T_g.[1] In the glassy region they have larger thermodynamic properties, such as volume or entropy, than those they would have in equilibrium state. Since the mobility of chain segments below T_g is not zero as revealed, for example, by volume relaxation studies,[2] there occurs a slow and gradual approach to equlibrium. Thus, the microstructure and consequently properties of the polymer change during annealing process in the temperature region where the polymer is in the glassy state. In other words, the physical state and properties of glassy polymers depend strongly on past sample

---

* 小谷　壽, 永田巨雄, 北村　昶, 根本紀夫, 倉田道夫 : Laboratory of Polymer Physical Chemistry, Institute for Chemical Research, Kyoto University, Uji, Kyoto 611.

history. This has been illustrated by effects of the annealing on density,[2] enthalpy,[3] and mechanical properties.[4] In general, the annealing range extends from T_g down to the highest secondary transition of the polymer.

Usually, small angle X-ray scattering and high resolution electron microscopy have been used to characterize the microstructure of polymers. However, even for semicrystalline polymers, an understanding of morphology at the molecular level can not be provided by these conventional methods alone. Furthermore, for nominally glassy polymers the problem of whether there exists local order, typically on a scale of $50 \sim 100$ Å, has not settled down yet.[5,6] Undoutedly analysis based on combined results employing various experimental techniques are needed to elucidate the complex microstructure of amorphous polymer solids.

The study of gas transport in polymers has contributed much to our understanding of the microstructure of polymers as well as that of the mechanism of diffusion.[7,8] Diffusion and solution behavior of simple gases are sensitive to both the morphology and molecular motion of the polymer on a scale comparable to the size of the penetrant molecule. Measurements can be made repeatedly using probe molecules of different sizes without perturbing the inherent sample properties. In addition, the fundamental dependence of transport and solution processes on the detailed nature of bulk polymers allows us to deduce the nature of certain changes in polymer microstructure which are not accessible to any other experimental method.

The present paper will describe transport studies of simple gases in atactic polystyrene which were undertaken to determine how does annealing in the glassy state of the polymer—sub-glass-transition aging—affect the transport and solution parameters, i.e. diffusion, permeation, and solubility coefficients, for simple gases. Also gas transport and solution data will be interpreted in conjunction with results obtained from dynamic mechanical measurements. Although for semicrystalline polymers, such as polypropylene, the microstructure and the morphological changes caused by the aging have been studied rather extensively by the gas transport and solution technique,[9-12] few studies have been made with amorphous polymers.

EXPERIMENTAL

Methods

Permeation experiments were performed by the partition cell method[13] in the temperature region from 23 to 130°C. The sample film which was supported from below by a piece of filter paper was placed on a drilled stainless steel plate and mounted in a permeation cell. The cell was divided into two chambers by the mounted film. The film and cell were throughly evacuated, then at time $t=0$, a known pressure p, from 5 to 25 cmHg, of the test gas was admitted to one side of the cell while essentially zero pressure was maintained at the opposite surface of the film. The increase in pressure with time in a constant-volume reservoir on the outgoing side of the film was measured by a rotary McLeod gauge. Measurements of the outgoing pressure were continued for a period at least three times longer than the time t' of nonlinear portion of the permeation curve. The steady-state permeation

was established after between 1.5 t' and 2 t' were elapsed.

The permeability coefficient P was calculated from the steady-state permeation rate J_s by the relation[7,8,14]

$$P = J_s(X/p) \qquad (1),$$

where X is the thickness of the film. The steady-state pressure increase in the reservoir was extrapolated to the time axis to give the time lag θ, and the diffusion coefficient D_θ was calculated by the relation[7,8,14]

$$D_\theta = X^2/(6\theta) \qquad (2).$$

The solubility coefficient S_θ was estimated through the relation

$$P = D_\theta S_\theta \qquad (3).$$

In Equations (2) and (3), the subscript θ means that the diffusion coefficient was determined from the time lag for permeation and that the solubility coefficient was calculated therefrom using the relation (3).

The dynamic mechanical measurements were performed with a torsion pendulum, based on the design of Kuhn and Kunzle,[15] at about a constant frequency of 0.1 Hz. Measurements were made in the temperature region from 30 to about 100°C at heating rate of 15°C/hr. The storage shear modulus and the loss tangent were determined from the oscillation period and the damping ratio, respectively, using the usual formulas.[16]

Materials

The polymer used in the present work was an anionically polymerized atactic polystyrene. The sample was generously provided by Professors S. Onogi and T. Masuda of this University. Purification and characterization of the sample have been described earlier.[17] The weight-average molecular weight, determined from the sedimentation equilibrium method, was 1.06×10^6. The ratio of weight-average to number-average molecular weight was estimated to be less than 1.05 from the sedimentation velocity boundary curve.

Films of the polymer were prepared by slow evaporation of solvent from a 5% dichloromethane solution on a clean mercury surface. Dichloromethane for spectroscopy, Merck Uvasol®, was used. Final traces of the casting solvent were removed by leaching in methanol for a week, followed by drying in a vacuum oven for more than 10 days at room temperature.

The films having different thermal histories were prepared by treating the films under different conditions as described below. After drying all the films were subjected to a thermal treatment at 130°C for 2 hr, then were divided into two groups. In the first group, films were cooled rapidly from 130 to 25°C. The quenched films were designated as sample A. Alternatively in the second group, films were subjected to subsequent annealing at 85°C for 10 days in a vacuum oven. The oven was then turned off and the films were left in the oven until they had cooled to room tem-

perature. The annealed films were designated as sample B.

The film thickness was determined by taking the arithmetic average of numerous readings of a micrometer screw aguge over the area of the film. Films used for gas transport and dynamic mechanical measurements were from 2.0×10^{-2} to 3.4×10^{-2} cm thick.

Inert gases of purity exceeding 99.995 vol % were used as probe molecule. These are helium, argon, and krypton. Also, methane of purity exceeding 99.7 vol % was employed as penetrant.

For every diffusion process of argon, krypton, and methane we were able to use a film giving a properly measurable time lag. Accordingly, diffusion coefficients were reproducible within about 15% for these systems. For diffusion processes of helium, however, even the thickest film was found to be too thin to get a proper value of time lag, e.g. something longer than five minutes. Therefore, determination of D was less accurate for helium diffusion, and the error in the determination was on average about 30%. Permeability coefficients were reproducible within about 12% for all systems studied.

RESULTS

For many gas-polymer systems it has been shown that the temperature dependence of gas transport parameters is influenced by the relaxation behavior of the polymer in the temperature region concerned.[7,8,18] Usually, a clear break in the Arrhenius plots of either P or D was observed at T_g of the polymer. Also, in some systems gas transport behavior in polymer exhibited a second transition in the glassy region of the polymer. In view of these results, will be shown first the mechanical relaxation data of two polystyrene samples which have been subjected to different thermal conditionings. Results of gas transport experiments will be given subsequently.

Mechanical Relaxation

Figure 1 shows the temperature dependence of the storage shear modulus G' and the loss tangent tan δ at about 0.1 Hz. For both samples, a relatively sharp rise in the mechanical loss curve was observed in the neighborhood of 90°C, and the rise was accompanied by a drop in the modulus curve. These changes are indicative of the relaxation mechanism associated with the primary glass-to-rubber transition of polystyrene.[19]

At all temperatures the annealed sample B exhibited a higher modulus than the quenched sample A. This indicates that the annealed sample is more rigid than the quanched one. Correspondingly, the latter showed a higher level in the loss curve than did the former.

In the loss curve for the sample A, a slight rise is seen in the vicinity of 65°C. The rise is presumably attributed to the so-called β transition—the secondary transition —of polystyrene.[20] For the sample B, on the other hand, no indication of the rise in the loss curve was observed in this temperature range.
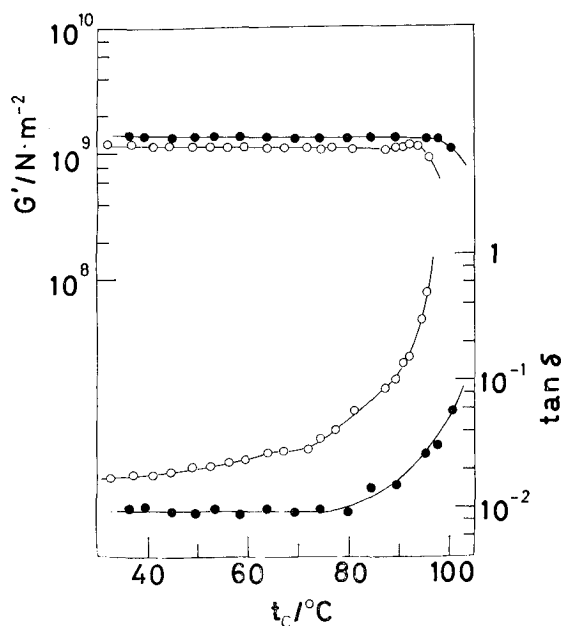
Fig. 1. Temperature dependence of the storage shear modulus G' and the loss tangent tan δ for polystyrene. $\bigcirc$: sample A; $\bullet$: sample B.

Permeation Behavior

The dependence of the permeability coefficients P on the ingoing pressures p was examined. For all systems studied, no dependence was observed under the experimental conditions.

In Fig. 2 the temperature dependence of P for helium in the quenched sample A is presented in the form of Arrhenius plot. The numbers associated with the data points represent the order in which they were determined. Points 22, 23, and 24,
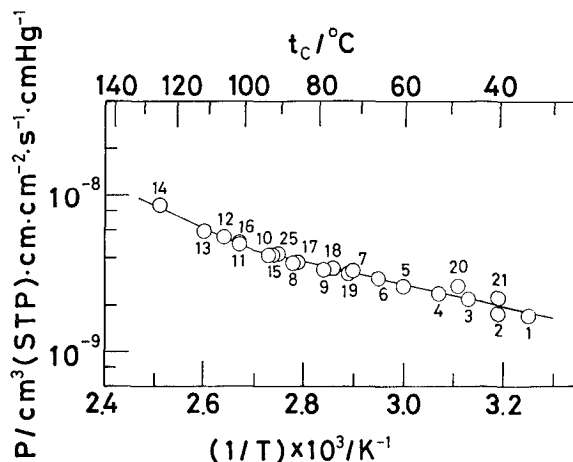

Fig. 2. Temperature dependence of the permeability coefficient P for helium in polystyrene (sample A).

(16)

which practically coincided with points 15, 7, and *2*, respectively, are not shown in the figure to avoid confusion.   It is seen that the order of determination has no effect on the values of *P*.

Though the data are not shown in the figure, plot for helium permeation in the annealed sample B was in good agreement with that for the sample A.   Accordingly, as far as the permeation behavior of gas molecules of small size like helium is concerned, it is concluded that the thermal history of polymer film has no effect on the behavior.

The Arrhenius plot is well represented by two straight lines which intersects at 97°C.   The temperature is close to the literature value of T_g for polystyrene.[21] The apparent activation energy for permeation is higher above T_g, and this has been observed usually for gas-polymer systems.[7,8,18]

The temperature dependence of *P* for argon, krypton, and methane are shown in Fig. 3, 4, and 5, respectively.   Contrary to helium permeation, the permeation behavior for these larger gases depends on the thermal history of the polymer film. Except for the data points for methane at lower temperatures, values of *P* for the quenched sample are higher than those for the annealed sample, and the difference becomes greater with increasing the size of the gas molecule.   Also, in no case can the plot for any gas be represented by two straight lines.   A somewhat flatter part is found in the vicinity of T_g.

An unusual behavior is seen in the plot for methane in the sample B.   Above the glass transition zone *P* dropped by a factor of about two with a small increase of temperature.   Also, a slight decrease of *P* with increasing temperature was observed at temperatures below about 65°C.   Usually the measurements were conducted by systematically increasing the temperature.   Even in results of this system, however, it was found that the permeation data obtained in a run of descending temperature were in agreement with those obtained in the preceding run within the average experimental error.   Since the permeability is a composite quantity as shown in
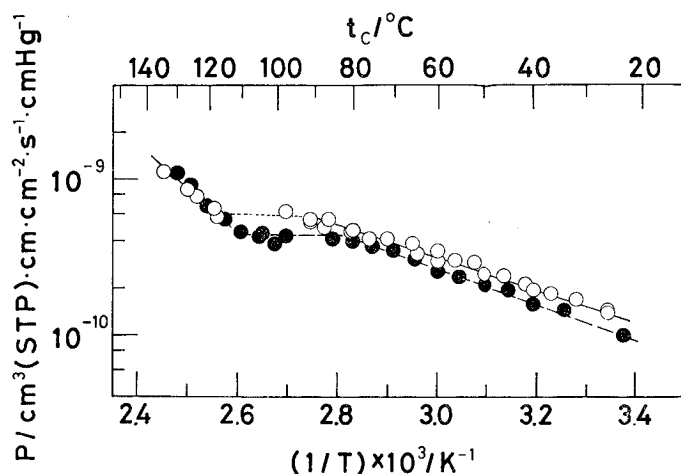

Fig. 3.   Temperature dependence of the permeability coefficient *P* for argon in polystyrene.   ○: sample A; ●: sample B.
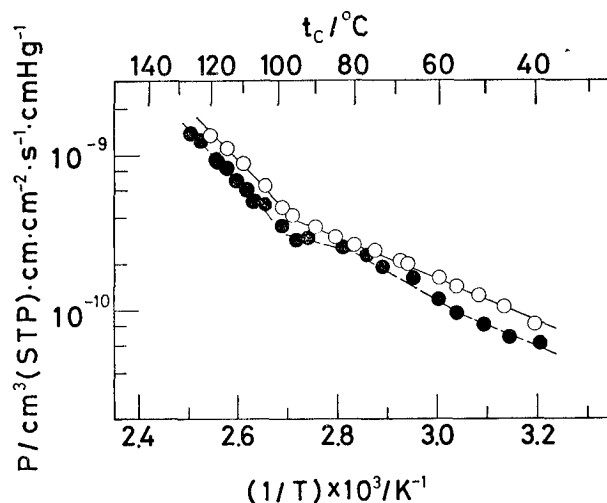
Fig. 4. Temperature dependence of the permeability coefficient P for krypton in polystyrene. $\bigcirc$: sample A; $\bullet$: sample B.
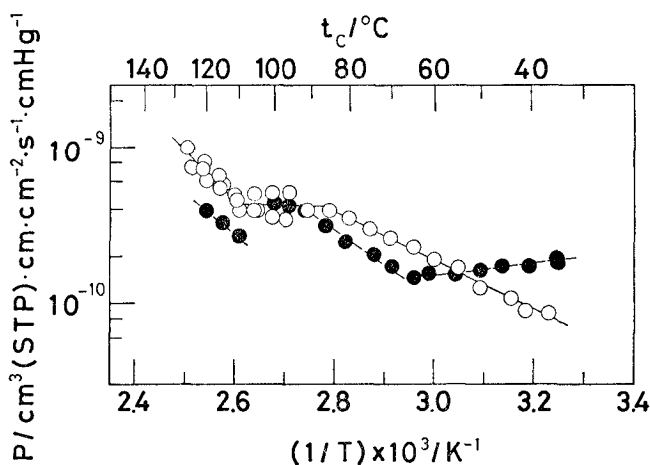

Fig. 5. Temperature dependence of the permeability coefficient P for methane in polystyrene. $\bigcirc$: sample A; $\bullet$: sample B.

Eq. (3), the anomalous behavior will be inspected below in terms of the temperature dependence of the diffusion and solubility coefficients.

Diffusion and Solubility Behavior

The temperature dependence of the time-lag diffusion coefficient D_θ and that of the solubility coefficient S_θ for helium are presented in Fig. 6. The plot of D_θ is represented by two straight lines of the form

$$D_\theta = D_0 \exp\left(-E_D/RT\right) \tag{4},$$

where the frequency factor D_0 and the activation energy for diffusion E_D are independent of temperature. The two straight lines intersect at a temperature in the
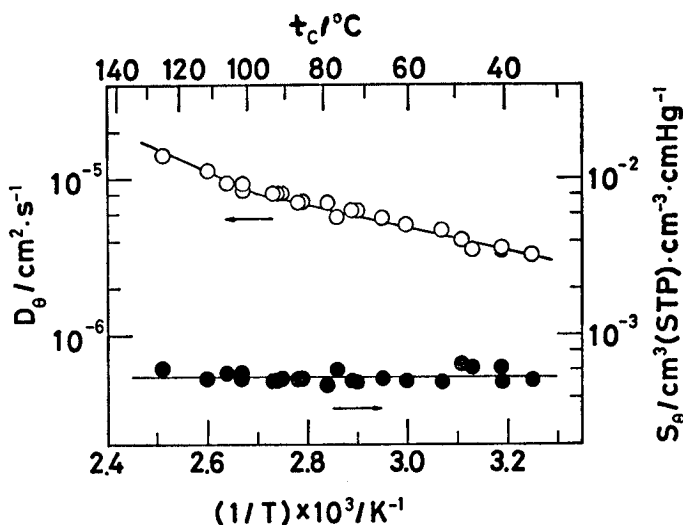
Fig. 6. Temperature dependence of the diffusion coefficient D_θ and the solubility coefficient S_θ for helium in polystyrene.

neighborhood of T_g. The plot of S_θ is expressed by single Arrhenius-type equation in the whole temperature range, that is,

$$S_\theta = S_0 \exp\left(-\Delta H_s / RT\right) \tag{5}.$$

Here ΔH_s is the apparent heat of solution. For helium solubility ΔH_s is observed as to be nearly zero.

The Arrhenius plots of D_θ and S_θ for argon, krypton, and methane are shown in Fig. 7, 8, and 9, respectively. In Fig. 9 are also shown diffusion data obtained by Lundberg et al. at temperatures above T_g.[22] It is seen that our results with the annealed sample B are compared well with theirs. For argon and krypton the plot of D_θ in the quenched sample at temperatures below T_g is in a higher level than that in the annealed sample. However, the opposite is the case for diffusion data of methane. For methane the diffusivity plot in the quenched sample is lower than that in the annealed sample over the whole region of temperature investigated.

For the three gases the diffusivity plot in the quenched sample is represented by two straight lines which intersect in the vicinity of T_g. While with the annealed sample, the experimental points lie on three distinct straight lines with two intersections. The upper intersection temperature agrees well with that of the diffusivity plot in the quenched sample, that is, the upper intersection temperature corresponds well to T_g. The lower intersection is less apparent compared with the upper one, and is indicated by an arrow sign in each figure.

Each solubility plot for the three gases in the quenched sample is represented by two straight lines. Surprisingly, the two straight lines do not intersect like diffusion data but a discontinuity is observed in the glass transition zone. Though the scatter is greater than that of data points of diffusion, or permeation, behavior, solubility coefficients above T_g seem to be nearly constant. A break is exhibited in the solubility
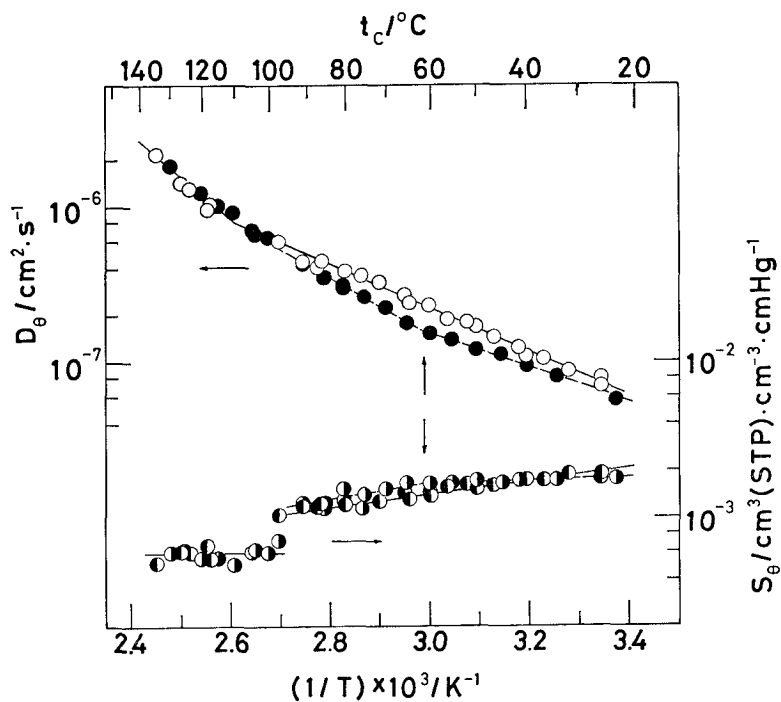
H. Odani, N. Nagata, N. Kitamura, N. Nemoto, and M. Kurata

Fig. 7. Temperature dependence of the diffusion coefficient D_θ and the solubility coefficient S_θ for argon in polystyrene. $\bigcirc$, $\pmb{\oplus}$: sample A; $\bullet$, $\pmb{\circ}$: sample B.
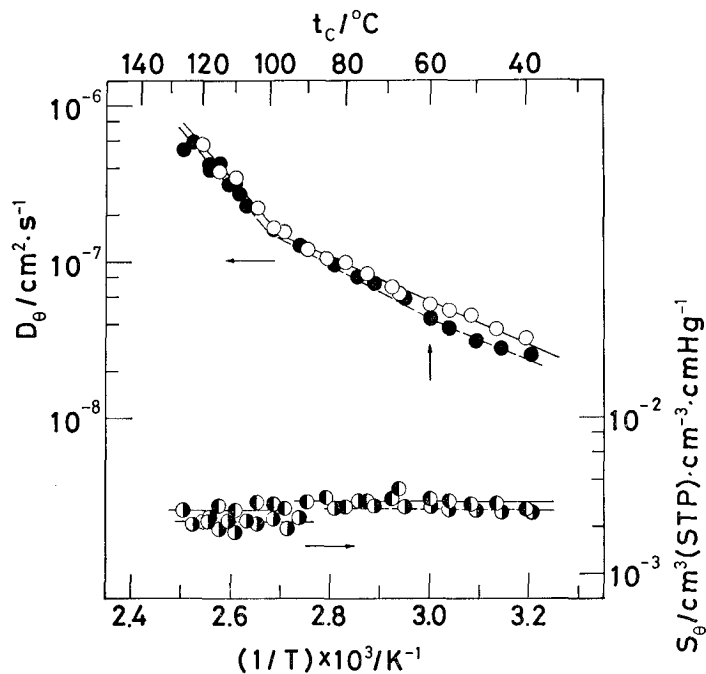
Fig. 8. Temperature dependence of the diffusion coefficient D_θ and the solubility coefficient S_θ for krypton in polystyrene. $\bigcirc$, $\pmb{\oplus}$: sample A; $\bullet$, $\pmb{\circ}$: sample B.
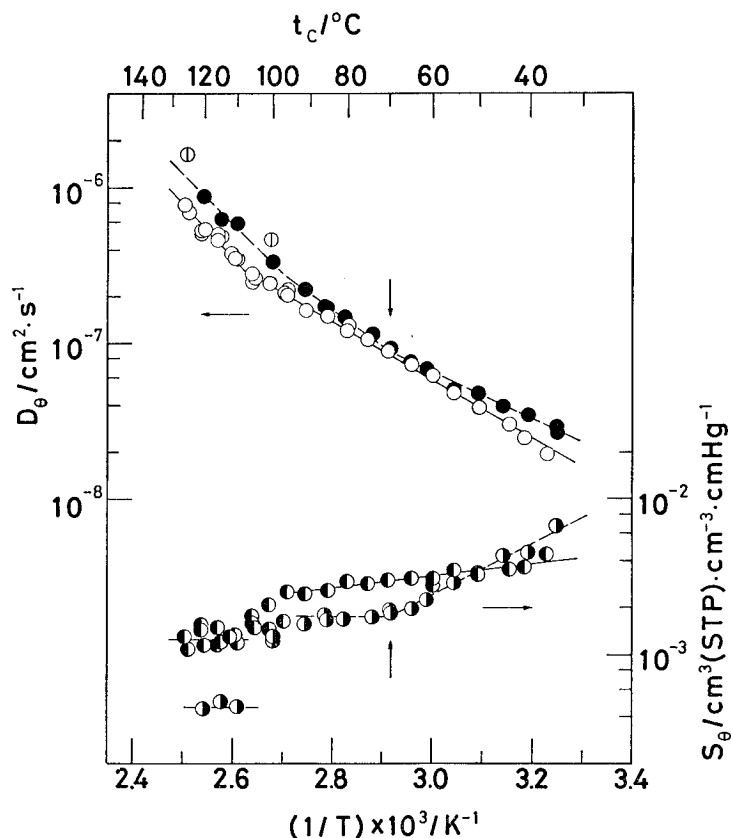
$t_c / {}^\circ C$

Fig. 9. Temperature dependence of the diffusion coefficient D_θ and the solubility coefficient S_θ for methane in polystyrene. $\bigcirc$, $\oplus$: sample A; $\bullet$, $\mathbb{O}$: sample B. $\oplus$: data obtained by Lundberg, Wilk, and Huyett[22].

plots below T_g for argon and methane in the annealed sample. The intersection point is also indicated by an arrow in each figure. The intersection temperature coincides well with the lower intersection temperature of the paired diffusivity plot. The lower intersection temperature T_b from the graphs are assembled in Table I. It is of interest to note that values of T_b are in the neighborhood of the literature value of the β transition temperature of polystyrene[20] quoted before.

In Table II are listed values of E_D and D_0. In every system the values of E_D

Table I. The lower intersection temperatures T_b for diffusion and solution in the annealed sample B.

Gas	$T_b/{}^\circ C$			
	He	Ar	Kr	CH$_4$
Diffusivity	—	61	60	70
Slubility	—	61	—	70

Table II. Activation energies E_D and values of D_0 for diffusion.

Gsa	Sample A		Sample B		
	$T<T_g$	$T>T_g$	$T<T_b$	$T_b<T<T_g$	$T>T_g$
	$E_D/\text{kJ}\cdot\text{mol}^{-1}$				
He	13.9	26.2	13.9		26.2
Ar	27.0	52.2	21.1	36.6	52.2
Kr	28.0	65.4	25.9	34.1	65.4
CH$_4$	36.3	63.2	29.1	42.6	64.6
	$D_0/\text{cm}^2\cdot s^{-1}$				
He	7.75×10^{-4}	4.11×10^{-2}	7.75×10^{-4}		4.11×10^{-2}
Ar	3.75×10^{-3}	1.01×10	3.03×10^{-4}	5.41×10^{-2}	1.01×10
Kr	1.36×10^{-3}	2.61×10^{-2}	4.90×10^{-4}	1.10×10^{-2}	2.86×10^2
CH$_4$	2.81×10^{-2}	1.36×10^{-2}	2.38×10^{-3}	2.77×10^{-1}	1.63×10^3

Table III. Heats of solution ΔH_s.

Gas	$\Delta H_s/\text{kJ}\cdot\text{mol}^{-1}$				
	Sample A		Sample B		
	$T<T_g$	$T>T_g$	$T<T_b$	$T_b<T<T_g$	$T>T_g$
He	~0	~0	~0		~0
Ar	-8.3	3.4	-0.2_1	-12.8	3.4
Kr	-2.0	0.3_5	0.4_8	1.3	0.3_5
CH$_4$	-6.3	0.3_8	-35.9	0	~0

increase with increasing temperature. Values of ΔH_s are given in Table III. As has been shown for many combinations of simple gas and amorphous polymer,[7,8] the values of ΔH_s are fairly small.

DISCUSSION

The differences observed in the modulus and the loss curves of the quenched and annealed samples may be qualitatively explained as the effect of thermal history on the density of the sample films. The sample quenched from the rubbery to the glassy state can be expected to be less dense than the sample annealed for a long period in the glassy state of the polymer. Because the quenched sample contains more free volume or holes, it will undergo, as it was warmed, the glass-to-rubber transition at somewhat lower temperature below T_g than will do the annealed sample. This is indeed what we observed for mechanical relaxation behavior of the two samples.

Since there are no transitions in the gases in the temperature region studied, the temperatures of the lower intersections in the diffusivity and solubility plots must reflect a change in the polymer medium. As mentioned previously, the intersection temperatures T_b are well compared with the β transition temperature of the polymer. It is of

interest that the secondary transition is revealed not only by the kinetic processes, diffusion and mechanical relaxation, but also by the equilibrium property of solubility. Concerning the effect of the thermal history of the polymer samples, the transition phenomenon is observed only with the annealed sample for diffusion and solubility behavior while it is exhibited only with the quenched sample for dynamic mechanical properties.

It has been proposed earlier that the β transition of polystyrene is due to phenyl ring rotation about the bond connecting the ring to the backbone of the polymer chain.[23] Another idea that the β transition is due to a Schatzki crankshaft or related type of motion has been presented.[24] These interpretations, however, are not supported by more recent investigations. A recent suggestion that the β transition arises from the local mode relaxation motion[25] accounts for most of the known facts. The effect of the thermal history on the appearance of the lower transition in diffusion, solubility, and mechanical relaxation behavior seems to be explained satisfactorily in terms of this mechanism. Since the transport behavior of simple gases are sensitive to the molecular motion of the polymer on smaller scale than are mechanical properties and also free volume content of the annealed sample is lower than that of the quenched sample, the observed effect of the thermal history may suggest that redistribution of the size of the fluctuating free volume elements would occur during the annealing process.

In the whole region of temperature investigated, it was found that the time-lag diffusion coefficients for smaller gases are higher than those for larger gases if a comparison is made at a given temperature. Also, no proportionality was found between the permeability coefficients and the reciprocals of the square root of molecular weight of the gas. These indicate that the transport processes of the gases are not controlled by the flow mechanism through micropores or channels existing in the bulk polymer structure but by the mechanism of the activated diffusion in condensed medium.

According to the activated diffusion process the holes need be formed when penetrant molecules diffuse through a polymer medium. It is obvious that for the diffusion of larger molecules, large holes should be formed in the polymer, which in turn will lead to high activation energy for diffusion. Brandt has presented a model for the diffusion of penetrant molecules in polymers and derived an expression for the activation energy for diffusion.[26] In this treatment, the activation energy is assumed to consist of two contributions: (a) an intermolecular energy term and (b) an intramolecular energy term. The former term is a function of the cohesive energy density of the polymer, and the diffusion process in rubbery polymers is considered to be governed mostly by this effect. Also, the intermolecular term depends on the diameter of the penetrant molecule. The latter term, on the other hand, is considered to arise from the bending of the two neighboring chains and is expressed as a function of the flexibility of the chain segment. For the diffusion in glassy polymers this intramolecular term dominates, and the activation energy is expressed as to be proportional to the square of the diameter of the penetrant molecule.

In Fig. 10 the measured activation energy for diffusion E_D with the annealed sample B in three ranges of temperature, i.e. above T_g, between T_g and T_b, and
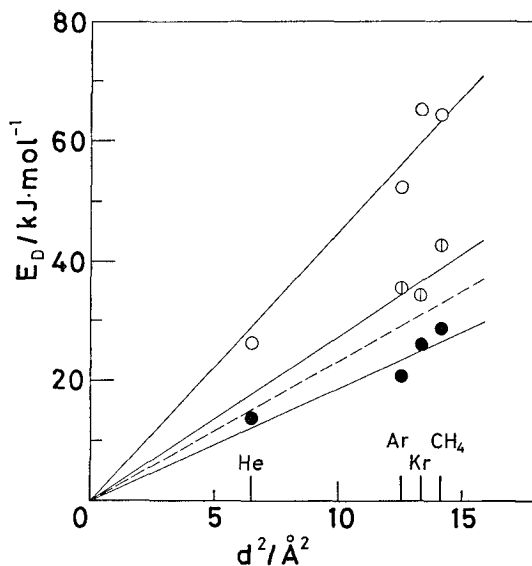
Fig. 10. Activation energy for diffusion in the sample B *versus* square of gas
diameter. $\bigcirc$: $T>T_g$, $\oplus$: $T_b<T<_gT$, $\bullet$: $T<T_b$; --- plot for
the sample A at temperatures below T_g.

below T_b, are plotted against to the square of the diameter of the gas molecule d^2.
Diameters of the gases at 25°C, which have been estimated from gas viscosities,[27]
were employed in the plots. It is seen that in every temperature range E_D cor-
relates well with d^2. Similar relations have been found by Meares for diffusion of
simple gases in polyvinyl acetate in the temperature region encompassing the glass
transition temperature of the polymer.[28]

Meares[28] has suggested that diffusion takes place along a somewhat cylindrical
volume equal to $(\pi/4)d^2\lambda$, where λ is the average path length of a diffusional step.
The activation energy for diffusion is given by

$$E_D = \frac{1}{4}\pi d^2 \lambda N_A E_C \qquad (6),$$

where N_A is the Avogadro number and E_C is the cohesive energy density of the polymer.
Using the slopes of the plots in Fig. 10 and the literature value of E_C for polystyrene,[29]
values of λ were estimated and summarized in Table IV. The path length for

Table IV. Path lengths for diffusion λ.

Gas	Sample A		Sample B		
	$T<T_g$	$T>T_g$	$T<T_b$	$T_b<T<T_g$	$T>T_g$
He	12.9	24.6		12.9	24.6
Ar	13.2	25.3	10.1	17.2	25.3
Kr	12.7	29.7	11.8	15.6	29.7
CH$_4$	15.6	27.2	12.4	18.3	27.6

diffusion, accordingly the size of zone of activation for diffusion, increases with increasing temperature. It is noted that for each gas the value of λ with the annealed sample is smaller than that with the quenched sample at temperatures below T_g. This also would suggest that the redistribution of the size of free volume elements may occur during the annealing period on the glassy state.

Meares also demonstrated a fundamental relationship between the energy and the entropy of activation.[28] The application of the theory of absolute reaction rates to diffusion[30] gives the expression of the diffusion coefficient D as

$$D = e\lambda^2 \frac{kT}{h} \exp\left(\frac{\Delta S^*}{R}\right) \exp\left(-\frac{E_D}{RT}\right) \tag{7}$$

where ΔS^* is the entropy of activation associated with a mole of unit diffusion acts, and e, k, and h have their usual meanings. Comparison with Eq. (4) shows that

$$D_0 = e\lambda^2 \frac{kT}{h} \exp\left(\frac{\Delta S^*}{R}\right) \tag{8}$$

Figure 11 shows relation between the entropy and the energy of activation for diffusion. At temperatures above T_g with both samples and at temperatures between T_g and T_b with the annealed sample, a linear relationship holds in each case.
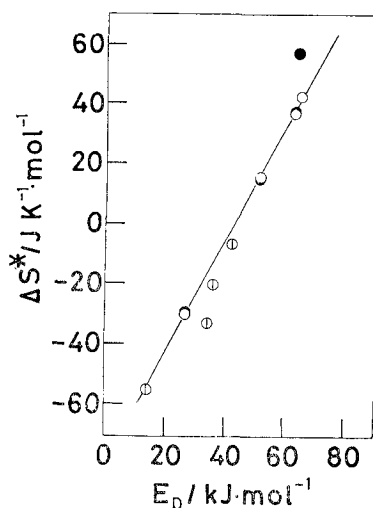

Fig. 11. Relation between entropy and energy of activation for diffusion.
○: sample A at 130°C $(T > T_g)$, ●: sample B at 130°C $(T > T_g)$,
⊕: sample B at 80°C $(T_b < T < T_g)$.

According to the theory developed by Gee[31] the logarithm of the solubility coefficient S of a gas in a polymer is correlated with the normal boiling point T_B of the gas through the formula

$$-\ln 76S = \left(\frac{\Delta S_v}{R}\right)\left(1 - \frac{T_B}{T}\right) - \ln\left(\frac{22400}{V_{dg}}\right) + 1 + \mu \tag{9}$$

where ΔS_v is the entropy of vaporization of the gas, V_{dg} is the molar volume of the dissolved gas, and μ is the Flory-Huggins interaction parameter. Also, heat of solution ΔH_s is given by

$$\Delta H_s = \mu RT + \Delta S_v T_B \qquad (10).$$

By assuming that Gee's relatinship is applicable to the time-lag solubility data in the glass transition zone, the equivalent molecular diameters d_g of the dissolved gas molecules were calculated from $(6V_{dg}/\pi)^{1/3}$ using the values of V_{dg}, which were estimated according to relationships Eq. (9) and (10). Table V lists the values of

Table V. Equivalent diameters of dissoleved gas d_g for solution.

| Gas | $d_g/\text{Å}$ | | | |
| | Sample A | | Sample B | |
	85°C $(T < T_g)$	130°C $(T > T_g)$	85°C $(T_b < T < T_g)$	130°C $(T > T_g)$
He	36.9	36.9	36.9	36.9
Ar	1.1	5.6	0.8	5.6
Kr	1.9	2.5	2.8	2.7
CH_4	1.1	3.0	2.6	3.5

d_g. Rather large values for helium suggests that a different molecular mechanism is operating in solution process of the gas. Presumably this correlates closely to the absence of the effect of thermal history on the transport and solubility behavior for helium. The values for the gases, except for helium, are of the same order of magnitude as van der Waals molecular diameters. At 85°C for krypton and methane, the values of d_g in the quenched sample are smaller than those in the annealed sample. Since the characteristic volume is determined by the molecular constraints imposed by the polymer matrix, this suggests again that the redistribution of the size of free volume elements may occur during the annealing process at temperatures between the primary and the secondary transition temperatures of the polymer.

REFERENCES

(1) G. Rehage and W. Borchard, in "The Physics of Glassy Polymers" R. N. Haward Ed., Applied Science Publishers, London, 1973, Chap. 1.
(2) A. J. Kovacs, *Fortschr. Hochpolym. Forsch.*, **3**, 394 (1964).
(3) S. E. B. Petrie, *J. Polym. Sci. Part A-2*, **10**, 1255 (1972).
(4) L. C. E. Struik, "Physical Aging in Amorphous Polymers and Other Materials", Elsevier, Amsterdam, 1978.
(5) P. Calvert, *Nature*, **271**, 507 (1978).
(6) *Faraday Disc. Chem. Soc.*, No. 68 (1979).
(7) C. E. Rogers, in "Physics and Chemistry of the Organic Solid State", Vol. 2, D. Fox, M. L. Labes, and A. Weissberger Eds., John Wiley & Sons, Inc., New York, 1965, Chap. 6.
(8) J. Crank and G. S. Park Eds., "Diffusion in Polymers", Academic Press, London, 1968.
(9) A. S. Michaels, H. J. Bixler, and H. L. Fein, *J. Appl. Phys.*, **35**, 3165 (1964).
(10) W. Vieth and W. F. Wureth, *J. Appl. Polym. Sci.*, **13**, 685 (1969).
(11) S. Kapur and C. E. Rogers, *J. Polym. Sci. Polym. Phys. Ed.*, **10**, 2107 (1972).

(12) A. H. Chan and D. R. Paul, *J. Appl. Polym. Sci.*, **24**, 1539 (1979); *Polym. Eng. Sci.*, **20**, 87 (1980); *J. Appl. Polym. Sci.*, **25**, 971 (1980).

(13) H. Odani, K. Taira, N. Nemoto, and M. Kurata, *Butl. Inst. Chem. Res., Kyoto Univ.*, **53**, 216 (1975).

(14) J. Crank, "The Mathematics of Diffusion", 2nd Ed., Clarendon Press, Oxford, 1975.

(15) W. Kuhn and O. Kunzle, *Helv. Chim. Acta*, **30**, 839 (1947).

(16) L. E. Nielsen, *Am. Soc. Test. Mat. Butl.*, No. 165, 48 (1950).

(17) N. Nemoto *Polym. J.*, **1**, 485 (1970).

(18) V. Stannett, *J. Membrane Sci.*, **3**, 97 (1978).

(19) K. Schmieder and K. Wolf, *Kolloid-Z.*, **134**, 149 (1953).

(20) R. F. Boyer, in "Encylopedia of Polymer Science and Technology", H. F. Mark, N. G. Gaylord, and N. Bikales Eds., Interscience, New York, 1970, Vol. 13, pp. 284–286.

(21) J. Brandrup and E. H. Immergut Eds., "Polymer Handbook", 2nd Ed., John Wiley & Sons, Inc., New York, 1975, p. III–154.

(22) J. L. Lundberg, M. B. Wilk, and M. J. Huyett, *I & EC Fundam.*, **2**, 37 (1963).

(23) K. H. Illers and E. Jenckel, *Rheol. Acta*, **1**, 322 (1958).

(24) R. F. Boyer, *Rubber Chem. Technol.*, **36**, 1303 (1963).

(25) O. Yano and Y. Wada *J. Polym. Sci. A-2*, **9**, 669 (1971).

(26) W. W. Brandt, *J. Phys. Chem.*, **63**, 1080 (1959).

(27) H. A. Stuart, "Die Struktur des Freien Moleküls", Springer-Verlag, Berlin, 1952, p. 83.

(28) P. Meares, *J. Am. Chem. Soc.*, **76**, 3415 (1954).

(29) H. Mark and A. V. Tobolsky, "Physical Chemistry of High Polymeric Systems", Interscience, New York, 1950, p. 263.

(30) S. Glasstone, K. J. Laidler, and H. Eyring, "The Theory of Rate Process", McGraw-Hill Book Co., New York, 1941, p. 516.

(31) G. Gee, *Quart. Rev.*, **1**, 265 (1947).